Controlled removal of individual carbon nanotubes from vertically aligned arrays for advanced nanoelectrodes†

Liangti Qu,*[a] Yang Zhao,[a] Yue Hu,[a] Han Zhang,[a] Yan Li,[a] Wei Guo,[b] Hongxia Luo[b] and Liming Dai*[c]

A simple but effective method has been developed to controllably extract carbon nanotubes (CNTs) from their vertically aligned arrays on growth substrates. The intrinsic micron-scale roughness of the CNT surface enables the protruding nanotubes to make good contact with an adhesive layer which can then remove them from the array on the growth substrate. This approach allows us to manage and tailor the surface morphologies and related surface properties of CNT arrays. The patterned structure of CNT arrays with region-selective control over the density has been achieved. The ability of this process to tailor spacing between vertically aligned CNTs, as demonstrated, opens a new pathway to fabricate the CNT nanoelectrode arrays for applications in electroanalysis.

1. Introduction

Vertically aligned carbon nanotubes (VA-CNTs) have captured considerable attention of scientists for years due to their unique electrical,[1,2] mechanical,[3] and optical[4] properties attractive for various applications, including in flat panel displays,[5] sensors,[6] actuators,[7,8] electronic devices,[9] smart polymer composites,[10,11] and even advanced dry adhesives.[12] For certain applications, effort may need to be made to not only control the structure of individual nanotubes but also their packing density to enhance their performance. In this regard, we, along with others, have devised many micropatterning methods, including photolithography,[13–15] soft lithography,[16,17] and electron or laser beam lithography[18,19] for producing uniform VA-CNT micropatterns. We have also achieved the formation of multicomponent VA-CNT micropatterns of multi-walled CNTs interposed with nanoparticles,[20] nonaligned CNTs,[21] or single-walled CNTs[22] by chemical absorption, self assembly, or direct chemical vapor deposition. On the other hand, considerable effort has been made to control the packing density of VA-CNTs for optimized field emission,[23,24] optoelectronic,[5] and electrochemical[25,26] performance in order to avoid the shielding effect associated with dense VA-CNT arrays. So far, methods used to form diluted VA-CNT arrays have mainly focused on reducing the catalyst site density for the nanotube growth by electron-beam lithography,[27] photolithography,[28] micro contact printing,[23] shadow mask,[29] and electrochemical deposition.[30] All of these methods require specific equipment with subtly controlled process for catalyst

patterning and nanotube growth. It will be of practical importance and a great advance if we could controllably extract nanotubes from their aligned arrays on the growth substrates. By doing so, we will be able to readily manipulate a preformed VA-CNT array, including the control of its packing density for diverse purposes.

While an innovative mechanical compression method to increase the CNT packing density has been recently reported,[31] no approach for decreasing the CNT packing density in a preformed VA-CNT array has been discussed in the literature. Herein, by selectively removing VA-CNTs from their growth substrate with a Scotch tape transfer method, we found that nanotube packing densities of preformed aligned CNT arrays can be readily tailored for various applications. By further combination with a conventional patterning technique, we also demonstrated that this simple method can be used not only to control the packing density of preformed VA-CNT arrays, but also to micropattern VA-CNTs with region-specific packing densities by region-selectively removing VA-CNTs. This, in turn, allows us to fabricate CNT nanoelectrode arrays that are attractive for high-performance electroanalysis.

2. Experimental

The VA-CNTs were prepared by pyrolysis of iron(II) phthalocyanine (FePc) on a quartz substrate with a size of ca. 1 cm × 1 cm under an Ar/H$_2$ flow at 800–1100 °C according to our reported procedures.[13,17,32] The CNTs have a tube length in the range 3–5 μm and a packing density of ∼10^9 per cm^2. To controllably remove the CNTs from their vertically aligned arrays, Scotch tape (3M) was placed flat on the CNT surface and covered with a glass slide, followed by a press of a certain force being applied to the glass surface. A lab balance underneath the CNT samples was used to determine the applied press force. Thereafter, the Scotch tape was peeled off quickly to selectively extract the CNTs from quartz substrate. The number of extracted CNTs strongly depends on the extracting cycles and applied press force. To form the CNT micropatterns with region-specific density, a TEM copper grid with a window size of ca. 40 μm was

[a]Department of Chemistry, School of Science, Beijing Institute of Technology (BIT), Key Laboratory of Cluster Science (Beijing Institute of Technology), Ministry of Education in China, Beijing, 100081, P. R. China. E-mail: lqu@bit.edu.cn; Fax: +86 10 68918608; Tel: +86 10 68918608
[b]Department of Physics, Renmin University, Beijing, 100081, P. R. China
[c]Department of Chemical Engineering, Case School of Engineering, Case Western Reserve University, Cleveland, OH, 44106, USA. E-mail: liming.dai@case.edu
† Electronic supplementary information (ESI) available: AFM of VA-CNT array and adhesive tape surface, and SEM images of extracted CNTs on adhesives. See DOI: 10.1039/c0jm00071j

placed between adhesive layer and CNT surface, followed by the extracting process. Polydimethylsiloxane (PDMS) film was formed by casting the dimethylsiloxane with curing agent (10 : 1 v/v) on a glass slide. After overnight curing under vacuum, the PDMS film was peeled off and used as a transfer substrate instead of Scotch tape for selectively extracting CNTs from the quartz substrate. Scanning electron microscopy (SEM) imaging was performed on a Hitachi S-4800 SEM unit. Optical transmittance of CNT samples were recorded on a U-3010 UV-vis spectrometer. The electrical resistance was measured by using a multimeter with a two probe distance of 1 cm. Atomic force microscopy (AFM) images were taken on a Nanoscope III MultiMode SPM (Digital Instruments) operated in tapping mode. Contact angles (CA) were measured on a Dataphysics OCA20 CA system at room temperature with distilled water (3 μL) as probe liquid. The average CA values were obtained by measuring more than five different positions of one sample. The electrical conductance and electrochemical measurement were performed with a CHI660B electrochemical working station. A three-electrode electrochemical cell was employed, consisting of the CNT electrode as the working (testing) electrode (effective size: 1 mm^2), a platinum wire (1.5 mm diameter) as the auxiliary electrode, and a silver wire (1.5 mm diameter) as the quasi-reference electrode.

3.   Results and discussion

Fig. 1 shows the procedure we used to controllably extract VA-CNTs from their growth substrates. The working principle lies on the selective contacts between the adhesive surface and the VA-CNT tips due to their intrinsic micro-scale roughness (Fig. S1†). Under an appropriate press force, only those nanotubes standing out from the top surface of VA-CNT arrays are preferentially contacted with the adhesive layer to be effectively removed from the substrate. As such, the packing density for the VA-CNTs that remained on the original substrate significantly reduced after this transfer process. By repeating this process, more and more VA-CNTs will be pulled off from the substrate to cause a gradual decrease in the nanotube packing density (Fig. 1).

In this study, we used the VA-CNTs synthesized by pyrolysis of iron phthalocyanine[32] on a quartz substrate, as an example, to demonstrate the method for selective removal of CNTs schematically shown in Fig. 1. The CNTs used as the starting materials have a tube length in the range 3–5 μm and a packing density of $\sim 10^9$ per cm^2. The interfacial adhesion force between the as-grown VA-CNT array and quartz substrate is about 20 N cm^{-2}. The interfacial force between the adhesive layer (Scotch tape) and VA-CNT top surface depends strongly on the pre-loading force applied, which can be regulated over a wide range from 0 to 50 N cm^{-2} with a pre-loading force of ca. 80 N cm^{-2}. Therefore, it is easy to remove all of the VA-CNTs from the growth substrate by simply pre-pressing Scotch tape hard onto a VA-CNT array to produce a much stronger adhesion to the Scotch tape than that with the growth substrate, as demonstrated in our previous publications.[20,33] In order to achieve the selective removal of VA-CNTs from the growth substrate, we applied a relatively low pre-loading force of ca. 4 N cm^{-2} onto a Scotch tape against the top surface of a VA-CNT array. By so doing, only the protruding VA-CNTs preferentially contacted with the adhesive layer will be pulled off from the growth substrate. Although the adhesion force between the VA-CNT array and the quartz substrate varies with the nanotube growth conditions, the much smaller area for active contacts of protruding VA-CNTs with the Scotch tape under a given pre-loading force (e.g. 4 N cm^{-2}) could dramatically enhance the adhesion between the Scotch tape and those protuberant VA-CNTs, which allows them to be selectively extracted from the growth substrate even with a relatively low apparent pre-loading force.

Fig. 2a shows four VA-CNT arrays on quartz substrates grown under the same conditions after having been subjected to different extracting times at a pre-loading force of 4 N cm^{-2}. As can be seen, the as-synthesized VA-CNT array is black and opaque. After four extracting cycles, the VA-CNT array became slightly semi-transparent. More extracting cycles caused the VA-CNT array to become more transparent (Fig. 2a, from left to right). The corresponding top-view SEM images show that the
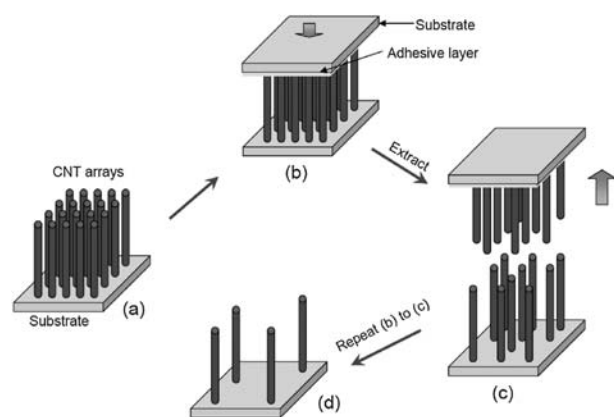
**Fig. 1**   Scheme showing the procedure to extract the CNTs from vertically aligned arrays.
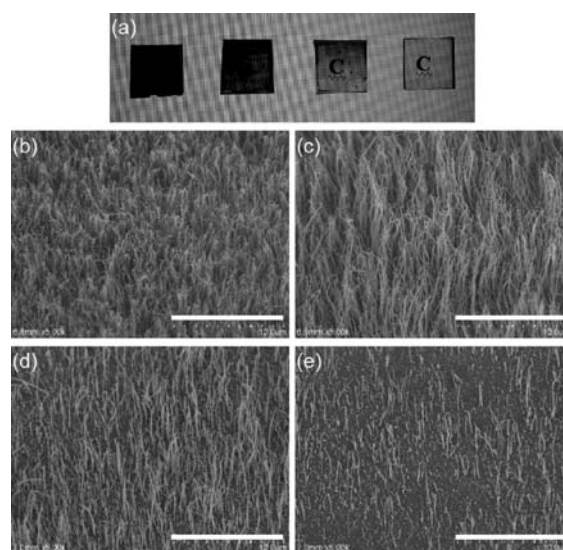
Fig. 2   Digital photo-image (a) of VA-CNT arrays on quartz substrates (ca. 1 cm^2) after 0, 4, 8, 12 extracting cycles (from left to right), and the corresponding SEM images (b–e) with a tilt angle of 30°. All scale bars represent 10 μm.
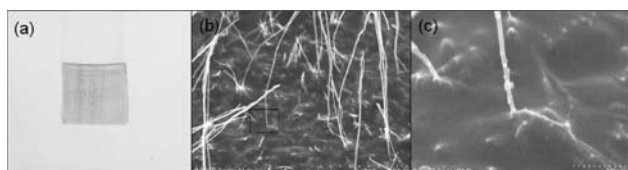
Fig. 3 Digital photo-image (a) of Scotch tape covered with CNTs pulled out from a VA-CNT arrays (highlighted in the squared area), and the corresponding SEM images (b, c) with a tilt angle of 45° with (c) being an enlarged view of the selected area in (b). Scale bars in (b) and (c) represent 5 μm and 500 nm, respectively.

initially compact VA-CNT array (Fig. 2b) became loosely packed (Fig. 2c) after several extracting cycles. The packing density of the VA-CNT array decreased with increasing extracting cycle number (Fig. 2d and 2e). It was also noted that the extracting process did not cause any obvious damage on the nanotube alignment due to the good mechanical properties intrinsically associated with the multiwall structure.[20] As highlighted in the squared area, Fig. 3a shows a digital photographic image for a Scotch tape covered with the CNTs extracted from a VA-CNT array. The corresponding SEM images revealed the transferred CNTs on the adhesive Scotch tape still stand up individually or in small bundles (Fig. 3b and Fig. S2†). As seen in Fig. 3c, the nanotubes have a firm contact with the Scotch tape by rooting themselves into the adhesive layer for a controlled removal from the growth substrate. The packing density of CNTs to be transferred onto the Scotch tape during each of the extracting cycles can be controlled by regulating the pre-loading force. By increasing the pre-loading force, we have indeed observed that an increasing number of CNTs were pulled off from the growth substrate (Fig. S2†). Therefore, the method developed in this study can be reliably used for controlled removal of CNTs from VA-CNT arrays.

As shown in Fig. 4a, a pseudo-linear decrease in the CNT density with increasing the extracting cycle number was observed. Consequently, the transparency of the VA-CNT
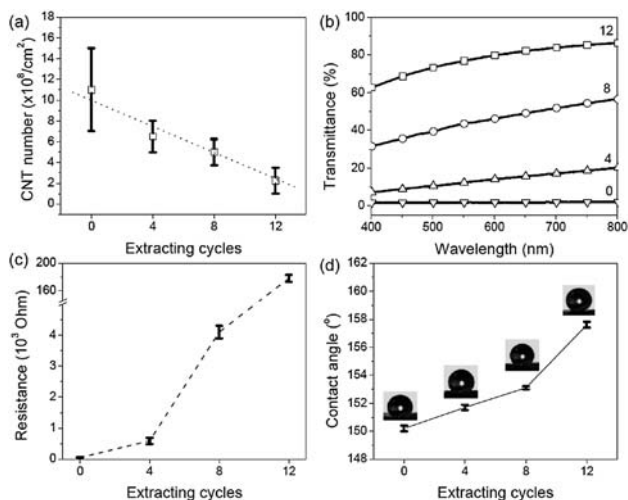
covered quartz substrate gradually increased with the increase of extracting cycles from 0 to 12 (Fig. 4b). The optical transmittance over 400–700 nm after 12 extracting cycles increased up to ~75% whereas the pristine sample is almost completely opaque. The corresponding electrical resistance increased with the increase in the extracting cycles due to the decreased CNT density on the quartz substrate (Fig. 4c). The dramatic resistance increase after about four extracting cycles is consistent with the disconnection among the VA-CNTs that remained on the growth substrate, as shown in the SEM images in Fig. 2. The increased spacing between CNTs caused by the extracting process allowed more air to be trapped within the CNT arrays. As a result, an increasing water contact angle was observed with increasing extracting cycles (Fig. 4d), leading to the superhydrophobic behavior.[34,35]

The extracting process, in combination with shadow lithography, enables us to achieve the region-selective density control. By placing a physical mask (e.g., TEM copper grid) between the adhesive layer and a VA-CNT array, the region-specific contact is effectively confined within the mask uncovered areas (Fig. 5a). As a result, the regions where the VA-CNTs have been selectively removed show a lower CNT density than that of their surrounding areas. Micropatterned VA-CNT structures on
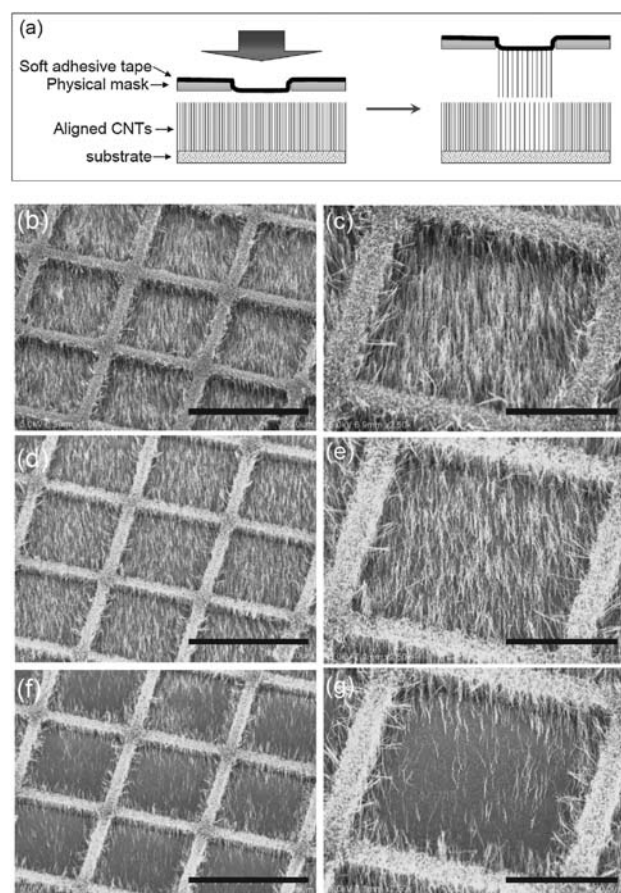
Fig. 5 A schematic representation of the procedure for the region-selective removal of VA-CNTs (a), and the resultant nanotube patterns of region-specific packing densities formed under different pre-loading forces: 10 (b, c), 20 (d, e), 30 (f, g) N cm⁻². Scale bars: left, 50 μm; right, 20 μm. (b) and (c), (d) and (e), (f) and (g) are from the same sample with different magnification.

Fig. 4 The CNT packing density (a), UV-visible spectra (b), electrical resistance (c) and surface wettability (d) of CNT samples after different extracting cycles.

quartz substrates with region-specific CNT density thus produced were shown in Fig. 5b, 5d and 5f. By controlling the pre-loading force applied, the extracting process combined with the physical masking can also be used to control VA-CNT micropatterns of different packing densities in each of the patterned regions. As can be seen in Fig. 5c, 5e, and 5g, changes in the pre-loading force from 10 to 30 N cm^{-2} produced patterned VA-CNTs of decreased CNT densities.

On the other hand, by using other flexible elastomeric (e.g., PDMS) films to replace the adhesive tape (Fig. 5a), we can produce CNT patterns with different CNT density on various substrates. Fig. 6 shows the micropatterns of CNT arrays with a tunable CNT density formed on PDMS films via the extracting process by simply changing the pre-loading force. As shown in Fig. 5a, the use of PDMS film instead of adhesive tape will allow the extracted CNTs to form the micropatterns on PDMS. Although there is no pre-coated adhesive layer on the PDMS film, the interfacial adhesion force[12,36] formed by pressing the PDMS film onto VA-CNT arrays under relatively high pre-loading forces (caption of Fig. 6) are sufficiently strong for pulling the VA-CNTs from the growth substrate. The formation of CNT micropatterns on PDMS with various packing densities could be useful for flexible electronics.[10]

The possibility of producing VA-CNT arrays with a tunable packing density prompted us to use this extracting approach to develop VA-CNT nanoelectrode arrays, in which each nanotube acts as an individual nanoelectrode without significant overlap of diffusion layers.[25] Fig. 7 schematically shows the fabrication procedure for the CNT nanoelectrode arrays. To start with, we fully coated the individually standing CNTs that remained on the SiO$_2$ substrate after the extracting process (Fig. 7a) with poly-styrene (PS, M_w = 350 000) by spin casting a ~15% solution of PS in THF. After one day drying in a vacuum oven at ambient temperature, the PS-coated VA-CNT array (Fig. 7b) was removed from SiO$_2$ substrate by etching the CNT-quartz inter-face with an aqueous HF solution (~10 wt%, Fig. 7c).[13] A thin layer of gold was then deposited onto the CNT tip-exposed side by sputtering (Fig. 7d). Thereafter, THF solvent was used to
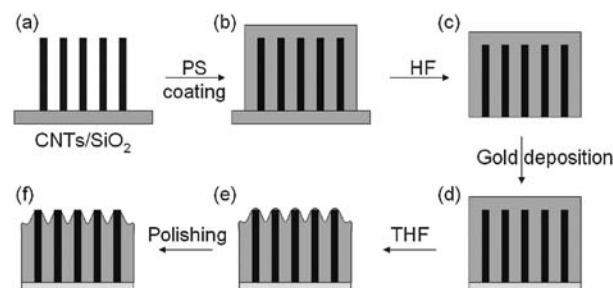

Fig. 7 Fabrication scheme of CNT nanoelectrode arrays.

carefully remove the redundant PS on the nanotube top end (Fig. 7e), followed by polishing the surface to expose the CNT tips using a fiber-free cloth (Fig. 7f). Finally, the sample surface was rinsed with deionized water, and the gold side was attached to the Cu wire by applying a drop of conductive silver epoxy followed by protection with an insulating epoxy coating. The PS-infiltrated VA-CNTs supported by a gold substrate thus prepared were then ready for subsequent electroanalysis.

For comparison, we also prepared VA-CNT array electrodes without extracting treatment. As expected, the pristine VA-CNT array electrode (Fig. 8a), corresponding to the sample in Fig. 2a, shows a much higher CNT density than the one after the extracting process (Fig. 8b). Unlike the pristine VA-CNT arrays with each of the constituent nanotubes closely packed together
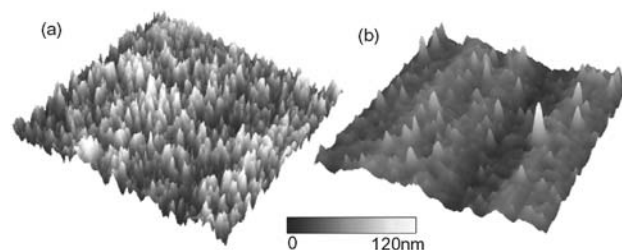

Fig. 8 AFM images of CNT electrode surfaces (5 × 5 μm) without (a) and with (b) extracting treatment.
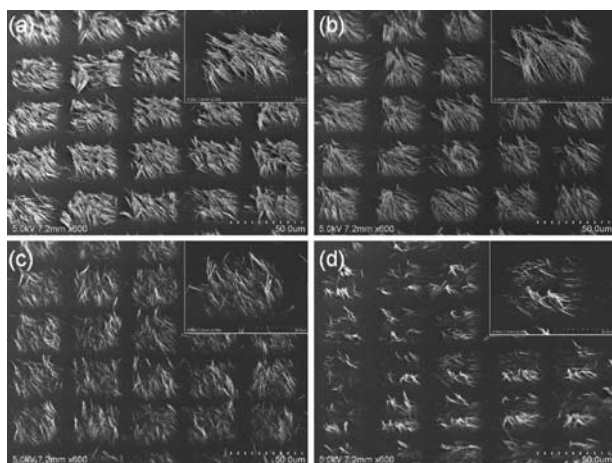

Fig. 6 Patterns of aligned CNTs transferred onto PDMS films under different pre-press forces ((a) 60; (b) 45; (c) 30; (d) 20 N cm^{-2}). Insets represent the enlarged view of a pattern unit (~2×). Inset scale bars represent 20μm.
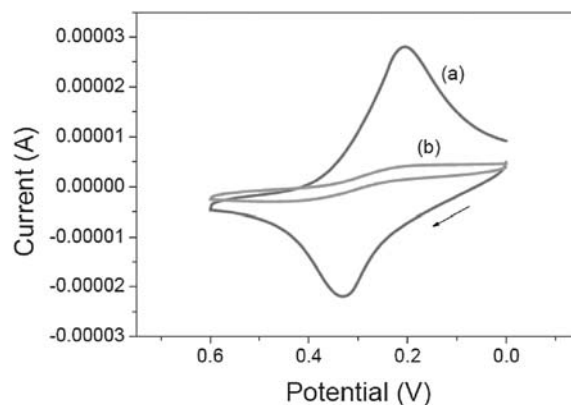

Fig. 9 Cyclic voltammetry (CV) curves of the CNT electrodes without (a) and with (b) extracting treatment as shown in Fig. 8. The CV curves were taken in a solution of 0.5 mM K$_3$Fe(CN)$_6$ in an aqueous solution of 0.1 M KCl. The scan rate was 50 mV s^{-1}. Sample size: 1 mm^2.

(Fig. 8a), each of the individual nanotubes in the nanoelectrode prepared by the extracting process stands up discretely (Fig. 8b).

To investigate the electrochemical properties, the cyclic voltammetric behavior of $K_3Fe(CN)_6$ was measured for the VA-CNT electrodes with and without the extracting treatment. For the pristine electrode with the densely-packed VA-CNT arrays (Fig. 9a), we observed the reversible anodic and cathodic peaks in the cyclic voltammograms attributable to electrochemical reactions of the $Fe(CN)_6^{4-}/Fe(CN)_6^{3-}$ redox couple. For the VA-CNT electrode after the lift-up process (Fig. 9b), however, the cyclic voltammograms show well-defined sigmoidal voltammetric curves characteristic of steady-state behavior at ultramicroelectrodes, apart from the considerably lower capacitance compared with the untreated sample (Fig. 9a) due to the much lower number of CNTs on electrode. These results suggest that the overlapping of diffusion layers associated with individual CNT nanoelectrode is dramatically eliminated in the VA-CNT electrode after the lift-up process and the behaviour of constituent CNTs is approaching to that of a microelectrode.

Conclusions

We have demonstrated a simple, but effective and versatile approach to selectively remove CNTs from VA-CNT arrays in a controllable fashion. The intrinsic micron-scale roughness of VA-CNT top surface and commercially available adhesive tapes enabled us to make selective contacts between protruding VA-CNTs and an adhesive layer for controllable removal of VA-CNTs from the growth substrate, which hence allows us to control and tailor the surface morphologies (e.g., density and patterns) and their related surface properties (e.g., optical, electrical, and hydrophobic behavior) of VA-CNT arrays. As demonstrated, this study opens up a new pathway to fabricate the CNT nanoelectrode arrays with each of the constituent VA-CNT acting as one single nanoelectrode, which is of great potential for electroanalysis particularly for electroactive species at low concentrations. We believed that the extracting methodology developed in this study could be applied to many other nanosystems beyond the CNTs.

Acknowledgements

References

1 J. W. G. Wilder, L. C. Venema, G. Rinzler, R. E. Smalley and C. Dekker, *Nature*, 1998, **391**, 59.
2 T. W. Odom, J. L. Huang, P. Kim and C. M. Lieber, *Nature*, 1998, **391**, 62.
3 A. Y. Cao, P. L. Dickrell, W. G. Sawyer, M. N. Ghasemi-Nejhad and P. M. Ajayan, *Science*, 2005, **310**, 1307.
4 M. J. O'Connell, S. M. Bachilo, C. B. Huffman, V. C. Moore, M. S. Strano, E. H. Haroz, K. L. Rialon, P. J. Boul, W. H. Noon, C. Kittrell, J. Ma, R. H. Hauge, R. B. Weisman and R. E. Smalley, *Science*, 2002, **297**, 593.
5 W. A. De Heer, A. Chatelain and D. Ugarte, *Science*, 1995, **270**, 1179.
6 P. G. He and L. M. Dai, *Chem. Commun.*, 2004, 348.
7 R. H. Baughman, C. Cui, A. A. Zakhidov, Z. Iqbal, J. N. Barisci, G. M. Spinks, G. G. Wallace, A. Mazzoldi, D. D. Rossi, A. G. Rinzler, O. Jaschinski, S. Roth and M. Kertesz, *Science*, 1999, **284**, 1340.
8 S. X. Lu, S. V. Ahir, E. M. Terentjev and B. Panchapakesan, *Appl. Phys. Lett.*, 2007, **91**, 103106.
9 W. B. Choi, B. H. Cheong, J. J. Kim, J. Chu and E. Bae, *Adv. Funct. Mater.*, 2003, **13**, 80.
10 Y. J. Jung, S. Kar, S. Talapatra, C. Soldano, G. Viswanathan, X. S. Li, Z. L. Yao, F. S. Ou, A. Avadhanula, R. Vajtai, S. Curran, O. Nalamasu and P. M. Ajayan, *Nano Lett.*, 2006, **6**, 413.
11 C. Wei, L. M. Dai, A. Roy and T. B. Tolle, *J. Am. Chem. Soc.*, 2006, **128**, 1412.
12 L. T. Qu, L. M. Dai, M. Stone, Z. H. Xia and Z. L. Wang, *Science*, 2008, **322**, 238.
13 Y. Yang, S. Huang, H. He, A. W. H. Mau and L. M. Dai, *J. Am. Chem. Soc.*, 1999, **121**, 10832.
14 C. Masarapu and B. H. Wei, *Langmuir*, 2007, **23**, 9046.
15 Z. J. Zhang, B. Q. Wei, G. Ramanath and P. M. Ajayan, *Appl. Phys. Lett.*, 2000, **77**, 3764.
16 Y. N. Xia and G. M. Whitesides, *Angew. Chem., Int. Ed.*, 1998, **37**, 550.
17 S. Huang, A. W. H. Mau, T. W. Turney, P. A. White and L. M. Dai, *J. Phys. Chem. B*, 2000, **104**, 2193.
18 H. Y. Wei, S. N. Kim, H. L. Marcus and F. Papadimitrakopoulos, *Chem. Mater.*, 2006, **18**, 1100.
19 W. H. Hung, R. Kumar, A. Bushmaker, S. B. Cronin and M. J. Bronikowski, *Appl. Phys. Lett.*, 2007, **91**, 093121.
20 J. B. Yang, L. T. Qu, Y. Zhao, Q. H. Zhang, L. M. Dai, J. W. Baur, B. Maruyama, R. A. Vaia, E. Shin, P. T. Murray, H. X. Luo and Z. X. Guo, *J. Nanosci. Nanotechnol.*, 2007, **7**, 1573.
21 J. Yang, L. M. Dai and R. A. Vaia, *J. Phys. Chem. B*, 2003, **107**, 12387.
22 L. T. Qu and L. M. Dai, *J. Mater. Chem.*, 2007, **17**, 3401.
23 L. Nilsson, O. Groening, C. Emmenegger, O. Kuettel, E. Schaller, L. Schlapbach, H. Kind, J.-M. Bonard and K. Kern, *Appl. Phys. Lett.*, 2000, **76**, 2071.
24 S. H. Jeong, H. Y. Hwang, K. H. Lee and Y. Jeong, *Appl. Phys. Lett.*, 2001, **78**, 2052.
25 Y. Tu, Y. Lin and Z. F. Ren, *Nano Lett.*, 2003, **3**, 107.
26 Y. H. Lin, F. Lu, Y. Tu and Z. F. Ren, *Nano Lett.*, 2004, **4**, 191.
27 Z. F. Ren, Z. P. Huang, D. Z. Wang, J. G. Wen, J. W. Xu, J. H. Wang, L. E. Calvet, J. Chen, J. F. Klemic and M. A. Reed, *Appl. Phys. Lett.*, 1999, **75**, 1086.
28 H. Murakami, M. Hirakawa, C. Tanaka and H. Yamakawa, *Appl. Phys. Lett.*, 2000, **76**, 1776.
29 S. Fan, M. G. Chapline, N. R. Franklin, T. W. Tombler, A. M. Cassell and H. Dai, *Science*, 1999, **283**, 512.
30 Y. Tu, Z. P. Huang, D. Z. Wang, J. G. Wen and Z. F. Ren, *Appl. Phys. Lett.*, 2002, **80**, 4018.
31 B. L. Wardle, D. S. Saiton, E. J. García, J. H. Hart, R. G. de Villoira and E. A. Verploegen, *Adv. Mater.*, 2008, **20**, 2707.
32 D. C. Li, L. M. Dai, S. Huang, A. W. H. Mau and Z. L. Wang, *Chem. Phys. Lett.*, 2000, **316**, 349.
33 S. M. Huang, L. M. Dai and A. W. H. Mau, *J. Phys. Chem. B*, 1999, **103**, 4223.
34 T. Sun, H. G. Wang Lin, L. Feng, L. Jiang and D. B. Zhu, *J. Am. Chem. Soc.*, 2003, **125**, 14996.
35 S. Li, H. Li, X. Wang, Y. Song, Y. Liu, L. Jiang and D. B. Zhu, *J. Phys. Chem. B*, 2002, **106**, 9274.
36 Y. Zhu, X. Lim, M. C. Sim, C. T. Lim and C. H. Sow, *Nanotechnology*, 2008, **19**, 325304.